Inhibition of Carbonic Anhydrase II by Thioxolone: A Mechanistic and Structural Study[†]

Albert A. Barrese, III,[¶,‡] Caroli Genis,[¶,§] S. Zoe Fisher,[§] Jared N. Orwenyo,[△,▽] Mudalige Thilak Kumara,[△] Subodh K. Dutta,[△,□] Eric Phillips,[△] James J. Kiddle,[△] Chingkuang Tu,[⊥] David N. Silverman,[§,⊥] Lakshmanan Govindasamy,[§] Mavis Agbandje-McKenna,[§] Robert McKenna,[*,§] and Brian C. Tripp[*,‡,△]

Department of Biological Sciences, Mailstop 5410, College of Arts and Sciences, 1903 West Michigan Avenue, Western Michigan University, Kalamazoo, Michigan 49008-5410, Department of Biochemistry and Molecular Biology, College of Medicine, P.O. Box 100245, University of Florida, Gainesville, Florida 32610-0267, Department of Chemistry, Western Michigan University, Kalamazoo, Michigan 49008-5410, and Department of Pharmacology and Therapeutics, College of Medicine, University of Florida, Gainesville, Florida 32610

Received December 6, 2007

ABSTRACT: This paper examines the functional mechanism of thioxolone, a compound recently identified as a weak inhibitor of human carbonic anhydrase II by Iyer et al. (2006) *J. Biomol. Screening 11*, 782−791. Thioxolone lacks sulfonamide, sulfamate, or hydroxamate functional groups that are typically found in therapeutic carbonic anhydrase (CA) inhibitors, such as acetazolamide. Analytical chemistry and biochemical methods were used to investigate the fate of thioxolone upon binding to CA II, including Michaelis–Menten kinetics of 4-nitrophenyl acetate esterase cleavage, liquid chromatography–mass spectrometry (LC-MS), oxygen-18 isotope exchange studies, and X-ray crystallography. Thioxolone is proposed to be a prodrug inhibitor that is cleaved via a CA II zinc-hydroxide mechanism known to catalyze the hydrolysis of esters. When thioxolone binds in the active site of CA II, it is cleaved and forms 4-mercaptobenzene-1,3-diol via the intermediate *S*-(2,4-thiophenyl)hydrogen thiocarbonate. The esterase cleavage product binds to the zinc active site via the thiol group and is therefore the active CA inhibitor, while the intermediate is located at the rim of the active-site cavity. The time-dependence of this inhibition reaction was investigated in detail. Because this type of prodrug inhibitor mechanism depends on cleavage of ester bonds, this class of inhibitors may have advantages over sulfonamides in determining isozyme specificity. A preliminary structure–activity relationship study with a series of structural analogues of thioxolone yielded similar estimates of inhibition constants for most compounds, although two compounds with bromine groups at the C1 carbon of thioxolone were not inhibitory, suggesting a possible steric effect.

Carbonic anhydrase (CA)[1] enzymes (EC 4.2.1.1) catalyze the reversible hydration of carbon dioxide to form bicarbonate and release a proton: $CO_2 + H_2O \rightleftarrows HCO_3^- + H^+$. CAs use a two-step "ping-pong" mechanism (*2–5*) that typically involves a zinc ion cofactor functioning as a Lewis acid to ionize a water molecule, although other metal ion cofactors are known (*6–8*). CAs are found in most eukaryotic and many microbial organisms (*9, 10*). There are currently five known CA structural families, the structurally characterized α-, *β*-, and *γ*-classes and the more recently discovered *δ*- and *ζ*-classes (*2, 7, 8, 11–15*). The zinc-dependent α-class CAs are the most clinically relevant family, with at least 14 known isoforms expressed in mammalian tissues (*11, 16–18*). First isolated and characterized in 1933 (*19, 20*), CA II is the most thoroughly characterized and fastest member of the α-class CA family, exhibiting near diffusion-limited kinetics (*3, 5, 21*). Mammalian α-CAs have important physiological functions including pH control, bicarbonate metabolism, and regulation of intracellular osmotic pressure (*22*). Consequently, a number of α-class CA isozymes, for example, CA II and CA IV, are the intended targets of drugs that function as CA inhibitors. CA inhibitors are commonly used as diuretics for the treatment of symptoms of hypertension (*23, 24*), as antiglaucoma drugs (*23, 25*), and for the treatment of high altitude sickness, gastric and

[†] This work was supported in part by a Thomas Maren Foundation grant (to R.M.) and a Small Investigator Grant provided by the Society of Biomolecular Screening (to B.C.T.).

[*] Corresponding authors. To whom correspondence should be addressed. (B.C.T.) Phone: (269) 387-4166. Fax: (269) 387-5609. E-mail: brian.tripp@wmich.edu. (R.M.) Phone: (352) 392-5696. Fax: (352) 392-3422. E-mail: rmckenna@ufl.edu.

[¶] A.A.B. and C.G. contributed equally to this work.

[‡] Department of Biological Sciences, Western Michigan University.

[§] Department of Biochemistry and Molecular Biology, University of Florida.

[△] Department of Chemistry, Western Michigan University.

[⊥] Department of Pharmacology and Therapeutics, University of Florida.

[▽] Current address: Chemistry Graduate Program, University of Maryland, Baltimore County, 1000 Hilltop Circle, Baltimore, MD 21250.

[□] Current address: Department of Chemistry, East Carolina University, Greenville, NC 27858-4353.

[1] Abbreviations: 4-NPA, 4-nitrophenyl acetate; CA, carbonic anhydrase; LC-MS, liquid chromatography–mass spectrometry; MWCO, molecular weight cut off; MRI, magnetic resonance imaging; PET, photon emission tomography; SAR, structure–activity relationship.

10.1021/bi702385k CCC: $40.75
Published on Web 02/12/2008

duodenal ulcers, epilepsy, memory function, and osteoporosis (*18, 23, 25, 26*). The CA IX and CA XII isozymes are also being investigated as potential targets of sulfonamide compounds for the treatment of certain types of cancers (*16, 23, 27*). Other uses being explored include treatment of osteoporosis and as a diagnostic tool in magnetic resonance imaging (MRI) and photon emission tomography (PET) (*25*). Furthermore, other α-class CA isozymes that may be therapeutically targeted by CA inhibitors are found in the prokaryotic mammalian pathogens *Neisseria gonorrheae*, (*28–30*) *Helicobacter pylori* (*31–33*), and the eukaryotic malarial parasite *Plasmodium falciparum* (*34–36*).

Known α-CA inhibitors include various anions, imidazole, phenol, hydroxyurea, carboxylates, organic phosphates and phosphonates, and various sulfonamide compounds (R-C-SO_2NH_2) (*4, 11, 25*). The first organic CA inhibitor discovered was sulfanilamide, a sulfonamide compound (*37*) and variations on the sulfonamide structure have yielded additional CA inhibitors, for example, sulfamates (R-OSO_2-NH_2), hydroxysulfonamides (R-$SO_2NH(OH)$), and hydroxamates (R-CO-NH-OH) (*11, 17, 38, 39*). To date, therapeutic CA inhibitors have been based on sulfonamide, sulfamate, and hydroxamate functional groups that coordinate to the active site zinc ion (*17, 23, 39–41*). Effective intraocular pressure reduction in the treatment of glaucoma requires large doses of sulfonamide drugs. These drugs often have poor specificity for the targeted isozyme, resulting in a wide array of undesirable side effects including altered taste, malaise, fatigue, depression, and anorexia (*42–45*). Furthermore, a significant fraction of the human population has demonstrated an allergic reaction toward some sulfonamide-based drugs (*46–48*). Thus, the discovery of new classes of non-sulfonamide CA inhibitors, potentially with more controlled specificity for different CA isozymes, could lead to the development of useful alternatives to existing drugs.

We recently performed a screening study of a model library of 960 structurally diverse, biologically active compounds against human CA II, using a well-known esterase assay with 4-nitrophenyl acetate (4-NPA) (*1, 49*−*52*). This screen yielded a number of CA inhibitors, including thioxolone (6-hydroxy-1,3-benzoxathiol-2-one), a biologically active compound not previously described as a CA inhibitor (compound **1**, Table 1). As reviewed by Byres and Cox (*53*), thioxolone has been classified as an antiseborrheic agent (*54*) and has been used in the treatment of skin conditions such as acne (*55*) and dandruff. Some hair-care products such as shampoos have incorporated thioxolone into their formulation as an antiseborrheic agent (*54*). Other reported medically useful properties include cytostatic, (*56*) antipsoriatic, antibacterial, and antimycotic activity; (*54*) some toxicity issues involving contact dermatitis have also been reported for this compound (*57*). The thioxolone structure is somewhat polar, with an XlogP value of 1.3, and has one hydrogen bond donor (a hydroxyl group) on one end and three hydrogen bond acceptors, including a carbonyl group on the other end, allowing for the formation of extensive hydrogen bonds (*53*). This structure lacks sulfonamide, sulfamate, or related functional groups that are typically a key structural feature of known CA inhibitors (*39*). Thus, it potentially represents a new class of lead compounds for further exploration and development as a non-sulfonamide therapeutic CA inhibitor.

Table 1: Structures and IC_{50} Values for Inhibition of Human Carbonic Anhydrase II by Acetazolamide and Thioxolone Analogues

Compound Number and Name	Molecular Structure	Molecular Formula	Mol. Mass (Da)	IC_{50} / K_i value (μM) [a,b]
1. thioxolone (6-hydroxybenzo[*d*][1,3]oxathiol-2-one)	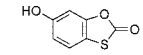	$C_7H_4O_3S$	168.2	*314 ± 69* [c] 1.77 [d] (1.06-2.95)
2. acetazolamide	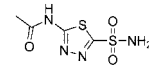	$C_4H_6N_4O_3S_2$	222.3	0.44 (0.42-0.47)
3. 4-mercapto-benzene-1,3-diol	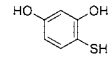	$C_6H_6O_2S$	142.2	*148 ± 39* [c] *n.d.* [e]
4. 2-hydroxythio-phenol	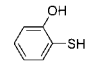	C_6H_6OS	126.2	*0.63 ± 0.03* [c] 1.05 (0.98-1.13)
5. benzenethiol	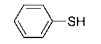	C_6H_6S	110.2	1.49 (1.28-1.74)

[a] IC_{50} values for inhibition of 4-NPA esterase kinetic rate, determined by absorbance measurements at 348 nm. [b] Error range for fitted IC_{50} value was defined as a 95% confidence interval. [c] Inhibitor constants (K_i values) for these compounds were determined using ^{18}O-exchange activity studies. [d] IC_{50} data from ref *1*. Error range for fit IC_{50} value was defined as a 95% confidence interval. [e] No data. No IC_{50} data was determined for this compound using the 4-NPA esterase assay.

The preliminary characterization of thioxolone inhibition indicated that it was a relatively weak CA II inhibitor, relative to some therapeutic sulfonamide inhibitors, both in a kinetic esterase assay with the substrate 4-NPA and in a competitive binding assay with the fluorescent probe, dansylamide. Thioxolone (compound **1**, Table 1) yielded an IC_{50} value of 1.8 μM and a K_d value of 33 μM vs an IC_{50} value of 0.31 μM and a K_d value of 20 nM for acetazolamide (compound **2**), a therapeutic CA inhibitor (*1*). The mechanism of CA II inhibition was not immediately obvious from the thioxolone structure. Phenol is a well-known CA inhibitor, (*58, 59*) and the C6 hydroxyl group of thioxolone could function in a phenol-like manner in binding to the zinc ion. The five-membered ring of thioxolone also contains both ester and thioester groups, which could mimic the transition state for the CA-catalyzed esterase reaction. Furthermore, either or both of the ester and thioester bonds could function as substrates for the well-known nonphysiological esterase activity of CA II, (*49, 50*) which involves a zinc-hydroxide mechanism (*49–52, 60–62*). Here, we describe a detailed initial investigation of the thioxolone inhibition mechanism, with the aim of gaining a more detailed understanding of this novel class of CA inhibitor, and present a set of structure–activity relationship (SAR) data for a number of structural analogues.

EXPERIMENTAL PROCEDURES

Enzyme Expression and Purification. The CA II expression plasmid, pACA, was a generous gift from Dr. Carol Fierke, University of Michigan. Bacterial expression and purification of CA II on a SP Sepharose Fast Flow (Amersham Biosciences/GE Healthcare, Piscataway, NJ) cation exchange column were performed as described previously (*1*). SDS−PAGE analysis indicated that the CA II had greater than 95% purity. The enzyme concentration was determined using a molar absorptivity of 5.4×10^4 M^{-1} cm^{-1}.

Materials. Pure analytical grade thioxolone (99% purity) and other chemicals and solvents were obtained from Sigma-Aldrich (St. Louis, MO), unless otherwise noted. The thioxolone hydrolysis product (compound **3**) was prepared by acid hydrolysis of thioxolone (Supporting Information). A set of 13 structural analogues of thioxolone, compounds **6**–**18** (Table 1) were obtained from Specs (Delft, Netherlands). Three other thioxolone analogues, compounds **19**–**21** (Table 1), were synthesized using thioxolone as a starting compound (Supporting Information).

Carbonic Anhydrase 4-NPA Esterase Inhibition Studies. The CA II esterase activity with 4-NPA as the substrate (*49*) has provided a reliable CA II activity assay that does not require the use of dissolved CO_2. The CA-catalyzed hydrolysis of 4-NPA results in the generation of a yellow 4-nitrophenolate anion with an isosbestic point at 348 nm that is readily detected with a spectrophotometer (*63*). IC_{50} values were determined using a 4-NPA esterase assay in 96-well microplates as previously described, (*1*) using 100 μL of assay solution containing 1 μM purified CA II in 50 mM, pH 7.5 MOPS, 33 mM Na_2SO_4, 1.0 mM EDTA buffer. The EDTA was added to minimize the background rate of solvent-catalyzed hydrolysis of the substrate. Thioxolone, 4-mercaptobenzene-1,3-diol, and other structural analogues were dissolved to a final concentration of 10 mM in 100% DMSO and were serially diluted 1:2 with pure DMSO in Costar 3365 round-bottom 96-well polypropylene plates (Corning, Lowell, MA). A volume of 1 μL of each compound was then transferred into the assay solution, using a CCS Packard PlateTrak robotic liquid handling system (PerkinElmer, Shelton, CT). The IC_{50} assays were determined in quadruplicate. Compounds were allowed to equilibrate with the enzyme for 15 min at room temperature. On each plate, the CA II inhibitor, acetazolamide (10 μM final concentration), was included as a positive control (100% inhibition) and 100% DMSO was included as a negative control (0% inhibition). The reaction was initiated by addition of 10 μL of 5.5 mM 4-NPA solution in 100% DMSO, with a Multidrop dispenser (MTX Laboratory Systems, Vienna, VA), and data collection was started. The absorbance of each well was measured at 348 nm every 15 s for 5 min with a SpectraMax Plus^{384} microplate spectrophotometer (Molecular Devices, Sunnyvale, CA), running SoftMax Pro software (version 4.8). The initial velocities, determined by the SoftMax Pro software, were normalized to a scale of 0% to 100% inhibition with an MS Excel spreadsheet, using the controls on each plate. This data were then fit using the GraphPad Prism (Version 4.03) graphing software to determine the IC_{50} values for each compound.

Michaelis–Menten Enzyme Kinetic Studies. A limiting concentration of enzyme was titrated against increasing concentrations of inhibitors. CA II was diluted with 50 mM pH 7.5 MOPS buffer, 33 mM Na_2SO_4, 1 mM EDTA, and 0.01% Triton X-100 in 1.5 mL disposable polystyrene cuvettes (Bio-Rad, Hercules, CA) and also in flat-bottom 96-well plates (Costar 3370), followed by addition of thioxolone (10 mM stock solution in 100% DMSO) to give a final enzyme assay concentration of 1 μM. The enzyme and thioxolone mixture was allowed to equilibrate for 15 min at room temperature, followed by addition of the 4-NPA substrate. The hydrolysis rate of 4-NPA was monitored by absorbance readings at 348 nm (A_{348}) with a Spectramax^{384} spectrophotometer in the kinetic data acquisition mode. Absorbance readings were collected every 9 s for 5 min, and initial data in the range of 5 to 30 s from each run were used to calculate the initial velocity, v_0. For the preincubation time studies, the enzyme and thioxolone mixture was allowed to equilibrate for one of seven different time periods (0 s, 1 min, 5 min, 10 min, 20 min, or 30 min), followed by rapid addition of the 4-NPA substrate with a pipettor. The hydrolysis rate of 4-NPA was then monitored by absorbance readings at 348 nm (A_{348}), with a SpectraMax Plus^{384} spectrophotometer in the kinetic data acquisition mode. Absorbance readings were collected every 2 s for an interval of 5 min, and initial data in the range of 5 to 30 s from each run were used to calculate the initial velocity, v_0. The $\Delta\varepsilon_{348}$ value used to calculate the 4-nitrophenolate ion product concentration at the isosbestic point was $5.0–10^3$ M^{-1} cm^{-1} (*64, 65*). The initial substrate concentration of 4-NPA was varied from 90 μM to 1.5 mM. As reviewed previously (*60, 62*), the solubility of the 4-NPA ester substrate is well below its K_M value for wild-type CA II, making it difficult to independently determine k_{cat} and K_M via a fit of the Michaelis–Menten equation. Instead, an apparent second order rate constant, k' ($=k_{cat}/K_M$), was calculated from initial slopes corrected for the background rate of hydrolysis, using the equation $v_0 = k'[E_0][S_0]$ (*62, 66*).

The time-dependent inhibition of CA II by thioxolone was investigated in greater detail by measuring initial rates of 4-NPA esterase hydrolysis after preincubation of the enzyme with thioxolone for varying times (0 s, 1 min, 5 min, 10 min, 20 min, or 30 min), at five different concentrations of inhibitor (10, 20, 50, 75, and 100 μM thioxolone) and with 750 μM 4-NPA initial concentration. Absorbance readings were again collected every 2 s for an interval of 5 min, and the initial data in the range of 5 to 30 s from each run were used to calculate the initial velocity, v_0. The apparent second order rate constant, k' ($= k_{cat}/K_M$), was again calculated from initial slopes corrected for the background rate of hydrolysis, using the equation $v_0 = k'[E_0][S_0]$. Then these k' values were used in a nonlinear regression analysis for a single phase exponential decay model, ($y = y_0 \exp(-kt) + y_{min}$, using GraphPad Prism 4.03) to determine the half-life of 4-NPA inhibition and the exponential decay constant. The intrinsic inactivation rate of thioxolone, k_{inact} was determined by nonlinear fitting of time-dependent data as a function of thioxolone concentration via the following equation: $k_{obs} = k_{inact}[I]/(K_I + [I])$, where k_{obs} is the exponential decay constant, k_{inact} is the intrinsic inactivation rate constant for thioxolone, [I] is the thioxolone concentration, and K_I is the equilibrium constant for thioxolone (*67, 68*) (Table 4).

Oxygen-18 Isotope Exchange Kinetic Inhibition Studies. Inhibition constants (K_i values) of thioxolone (compound **1**), 4-mercaptobenzene-1,3-diol (compound **3**), and 2-hydroxythiophenol (compound **4**) were determined by measurement of the inhibition of the ^{18}O-exchange activity between CO_2 and water via mass spectrometry, as reviewed elsewhere (*69, 70*). Experiments were carried out at 25 °C in solutions buffered at pH 7.4 with 0.1 M Hepes. The total concentration of all species of CO_2 was 10 mM, and the enzyme concentration was 7.3 nM. Inhibitor concentrations

ranged up to 800 μM and were analyzed by the method of Henderson for tight binding inhibitors (*71*).

Liquid Chromatography–Mass Spectroscopic Studies. Thioxolone cleavage in the presence and absence of CA II was analyzed by liquid chromatography–mass spectrometry (LC-MS). The CA II-thioxolone sample was prepared by first mixing 5 μM thioxolone (final concentration) with 5 μM CA II (final concentration) and 50 mM MOPS, pH 7.5, 33 mM Na_2SO_4 and 1 mM EDTA buffer to bring the total volume to 5 mL in a 15 mL round-bottom centrifuge tube. After being mixed by vortexing briefly for 30 s, the reaction was allowed to proceed at room temperature for 1 h. After 1 h, the sample was pipetted into a 2 mL 10 kDa molecular weight cut off (MWCO) Centriplus centrifugal dialysis concentrator (Millipore, Bedford, MA) and centrifuged at 4500*g* until most of the sample had passed through (approximately 1 h). The purpose of this step was to remove the CA II enzyme from any potential hydrolysis products. A stock solution of 10 mM thioxolone in 100% DMSO was diluted into 50 mM MOPS, pH 7.5, 33 mM Na_2SO_4, and 1 mM EDTA buffer to a final concentration of 5 μM (5 mL total volume) to prepare the enzyme-free control sample. Both samples were then adjusted to an approximate pH of 3 by dropwise addition of 1:10 diluted HCl (1.24 M), checking the pH after every few drops with pH strips to ensure that the pH was not too low. After the pH was adjusted, an equal volume of HPLC-grade chloroform was added into the tube and then vortexed vigorously for 1 min. After each tube had been vortexed once, the tubes were vortexed a second time to ensure complete mixing. The samples were then allowed to settle, resulting in phase separation of the chloroform from the aqueous layer. The aqueous layer was then removed with a Pasteur pipet. After the aqueous layer was removed, the tube was quickly vortexed for a few seconds and allowed to settle, checking for the presence of the remaining aqueous phase. This process was repeated for each sample. After all of the aqueous layers were removed, the samples were transferred to a clean small glass vial and were placed into a vacuum desiccator to remove the chloroform. Following complete removal of the chloroform, 1 mL of HPLC-grade methanol was added to each vial and samples were vortexed to resuspend the remaining residue. The samples were then filtered through a 0.2 μM pore size filter and stored in 1.5 mL microcentrifuge tubes at 4 °C if not used immediately.

The resulting thioxolone hydrolysis samples were analyzed on Shimadzu 2010A LC-MS instrument (Shimadzu Scientific Instruments, Columbia, MD) equipped with a manual injector, LC pumps, a photo diode array (PDA) detector, and an electrospray ionization (ESI) probe. All samples were dissolved in methanol. Sample introduction was achieved by direct manual injection of a 5 μL sample solution with the methanol mobile phase pumped at an isocratic flow rate of 0.6 L/min. Sample ionization was achieved by electrospray ionization (ESI) in negative polarity mode with a 1 s event scan time. Ionization parameters include a nebulizer gas flow rate of 2.5 L/min, a detector voltage of 1.5 kV, and a curved desolvation heater temperature of 250 °C.

X-ray Crystallographic Studies of CA II Complexed with Thioxolone and 2-Hydroxythiophenol. The hanging-drop vapor diffusion method was used to grow wild-type CA II crystals at room temperature (*72*). The crystallization drops for the crystals soaked with thioxolone (compound **1**) were prepared by mixing 8 μL of protein ($\sim$10 mg mL^{-1} in 50 mM Tris-HCl pH 7.8) with 2 μL of precipitant solution (50 mM Tris-HCl pH 8.0, 2.6 M ammonium sulfate). The crystallization drops for the crystals soaked with 2-hydroxythiophenol (compound **4,** Oakwood Laboratories, Oakwood Village, OH) were prepared by mixing 9 μL of protein ($\sim$10 mg mL^{-1} in 50 mM Tris-HCl pH 7.8) with 1 μL of precipitant solution (50 mM Tris-HCl pH 9.0, 1.3 M sodium citrate). Both conditions were equilibrated against 1 mL of their respective precipitant solution. Useful crystals in the ammonium sulfate condition appeared within 5 days, and useful crystals in the sodium citrate condition appeared within 8 days.

CA II crystals obtained using ammonium sulfate as the precipitant were incubated with 2 μL of thioxolone (20 mM in 50% DMSO) at room temperature in 10 μL of stabilizing solution for $\sim$24 h prior to data collection, whereas the CA II crystal obtained using sodium citrate as the precipitant was soaked with 2 μL of 2-hydroxythiophenol (20 mM in 50% DMSO) also at room temperature with 10 μL of precipitant solution for $\sim$24 h prior to data collection.

Both X-ray diffraction data sets were collected to 1.6 Å resolution at room temperature, using an R-AXIS IV++ image plate system with osmic mirrors and a Rigaku HU-H3R Cu rotating anode operating at 50 kV and 100 mA. The crystal-to-detector distance was set to 120 mm during the data collection with a 1° oscillation angle with 8 min exposures per image. X-ray data indexing was performed using DENZO and scaled and reduced with SCALEPACK (*73*). Both crystals were shown to be isomorphous to previously grown CA II crystals and belonged to space group $P2_1$ with mean unit cell dimensions: $a = 42.8 \pm 0.1$, $b = 41.7 \pm 0.1$, $c = 73.0 \pm 0.1$ Å, and $\beta = 104.7 \pm 0.1°$. Details of data collection and processing are given in Table 3.

The structures were phased using molecular replacement methods with the software package, Crystallography and NMR Systems (CNS) (*74, 75*). The structure of HCA II (PDB accession code: 1TBT), with the solvent molecules removed, was used as the search model (*70*). After one cycle of rigid body refinement, annealing by heating to 3000 K with gradual cooling, geometry-restrained position refinement, and temperature factor refinement, $F_o - F_c$ Fourier electron density omit maps were generated (Figures 2 and 3). Using the computer-graphics program Coot, (*76*) the residual density of these maps were interpreted, and the positions of the complexed molecules were built. The PRODRG (http://davapc1.bioch.dundee.ac.uk/programs/prodrg/) server was used to build coordinate and topology files for the molecules built (*77*).

A second cycle of CNS refinement, with the complexed molecules built, resulted in an R_{work} and R_{free} of 0.183 and 0.285 for thioxolone soaked crystal, and 0.232 and 0.265 for the 2-hydroxythiophenol complex. Subsequently, the refinements were continued using SHELXL97 in the conjugate-gradient least-squares mode (CGLS) with SHELXL default restraints, (*78*) followed by manual remodel building with the computer-graphics program COOT (*76*). The water molecules were added for both structures. Refinement of the structures continued until R_{cryst} and R_{free} converged. The final R_{cryst} and R_{free} were 0.164 and 0.211, and 0.187 and 0.220 for the thioxolone and 2-hydroxythiophenol soaked crystals, respectively. The occupancy for all atoms (including com-

Table 2: Michaelis–Menten Kinetic Parameters Determined for Concentration-Dependence of Thioxolone Inhibition of 4-Nitrophenyl Acetate Hydrolysis by Carbonic Anhydrase II[a]

thioxolone concentration (μM)	0	25	50	99
		Best-Fit Values		
k_{cat} (s^{-1})	2670	1530	914	734
K_M (mM)	1.13	1.17	1.50	2.08
		Std Error		
k_{cat} (s^{-1})	521	1130	748	577
K_M (mM)	0.32	0.81	0.93	1.21
		95% Confidence Intervals		
k_{cat} (s^{-1})	1600 to 3740	−798 to 3860	−630 to 2460	−452 to 1920
K_M (mM)	0.48 to 1.78	−0.48 to 2.81	−0.40 to 3.39	−0.37 to 4.52
R^2	0.97	0.84	0.91	0.95

[a] Kinetic measurements of thioxolone inhibition of the 4-NPA esterase reaction were performed using 1 μM CA II, as described in Experimental Procedures. GraphPad Prism version 4.03 was used to fit the data.

pounds 4-mercaptobenzene-1,3-diol, *S*-(2,4-thiophenyl)hydrogen thiocarbonate, 2-hydroxythiophenol, and solvent molecules) were fixed at 1.0 during refinement. The ligand−enzyme interactions were determined with LIGPLOT, and the model geometries were analyzed by PROCHECK (*79, 80*). All data-refinement and final model statistics are given in Table 3.

The final, refined models and experimental data have been deposited with the Protein Data Bank, with PDB accession codes 20SF and 20SM for the CA II crystal soak with thioxolone (complexed with 4-mercaptobenzene-1,3-diol (compound **3**) and *S*-(2,4-thiophenyl)hydrogen thiocarbonate) and 2-hydroxythiophenol (compound **4**), respectively.

RESULTS

Enzyme Kinetic Studies. Michaelis–Menten kinetics were measured for the rate of 4-NPA ester hydrolysis by CA II as a function of thioxolone concentration, to determine possible mechanisms of inhibition. The upper limit of substrate concentration (0.5 mM) was within the typical range of 0.4 to 1.0 mM 4-NPA concentration used in CA activity assays (*1, 52, 65*) and is far in excess of the enzyme concentration (1 μM). The substrate concentration is well below experimental estimates of K_M for this enzyme–substrate combination, which, because of the relatively low solubility of 4-NPA in aqueous solution, vary between 4 and 22 mM (*52, 81*). However, the chosen range of 4-NPA substrate concentrations well below K_M should also yield good sensitivity for detection and monitoring of potentially weak competitive inhibitors of the system (*82*), such as thioxolone.

The CA II-catalyzed 4-NPA esterase reaction rate was dependent on the concentration of thioxolone (Figure 1a); the initial reaction velocity decreased with increasing thioxolone concentration, confirming inhibition by this compound. The best-fit values of the Michaelis–Menten parameters, k_{cat} and K_M, decreased and increased, respectively, as the concentration of thioxolone was increased (Table 2). These results are suggestive of a mixed inhibition mode (i.e., competitive and noncompetitive), a result further supported by a Lineweaver–Burke plot analysis of the kinetic data (Figure 1a, inset). However, these results do not exclude a purely competitive mode of inhibition, as the range of substrate concentrations used was well below the K_M value, for reasons discussed above. It should also be noted that the 4-NPA assay used a nonphysiological esterase reaction with a substrate that has a relatively large aromatic group; however, there is considerable evidence that both esterase and CO_2 hydration reactions use the same zinc hydroxide mechanisms (*52, 62*).

Additional kinetic studies also clearly indicated that thioxolone exhibited time-dependent inhibition of the CA II esterase reaction, but that the majority of inhibition occurred within the 15 min preincubation period used for all IC_{50} experiments with 4-NPA substrate (Figure 1b). A fit of the apparent second order rate constant, k', as a function of thioxolone preincubation time, to a single exponential decay model, yielded an estimated half-life for inhibition of 4-NPA esterase activity of 340 s. The nonlinear fit of time-dependent data as a function of thioxolone concentration can be seen in Figure 1c and the k_{inact} and K_I parameter values (Table 4).

X-ray Crystallography of Thioxolone Compounds with Carbonic Anhydrase II. The refined crystal structure for the CA II crystals soaked with thioxolone (compound **1**) revealed a number of unexpected results (Figure 2). The most surprising result was the observation that thioxolone was not present in the crystal, but rather the thioxolone had been hydrolyzed into the ester product 4-mercaptobenzene-1,3-diol (compound **3**) and was directly bound to the active site zinc via coordination by the C3 thiol group (Figure 2b). The carbon ring was further stabilized via Van der Waals interactions with residues Val121, Leu198, and His94. This result immediately suggested that the thioxolone structure was readily cleaved into the ester hydrolysis product via an active site zinc-hydroxide mechanism, as hypothesized for other esters (*52*). In addition to the presence of 4-mercaptobenzene-1,3-diol (compound **3**) in the CA II active site, a catalytically hydrolyzed intermediate, *S*-(2,4-thiophenyl)hydrogen thiocarbonate, was observed at the rim of the CA II active-site cavity (Figure 2c). The carboxyl group was pointed toward the active site, stabilized by several solvent molecules, and the carbon ring was stabilized via Van der Waals interactions with residues Ile91 and Asp72 (Figure 2c).

These structural results raised a number of questions that we attempted to address in the further analytical chemistry, kinetics, and structural experiments. Further crystallographic studies yielded the structure of CA II complexed with 2-hydroxythiophenol (compound **4**) (Figure 3). This structure

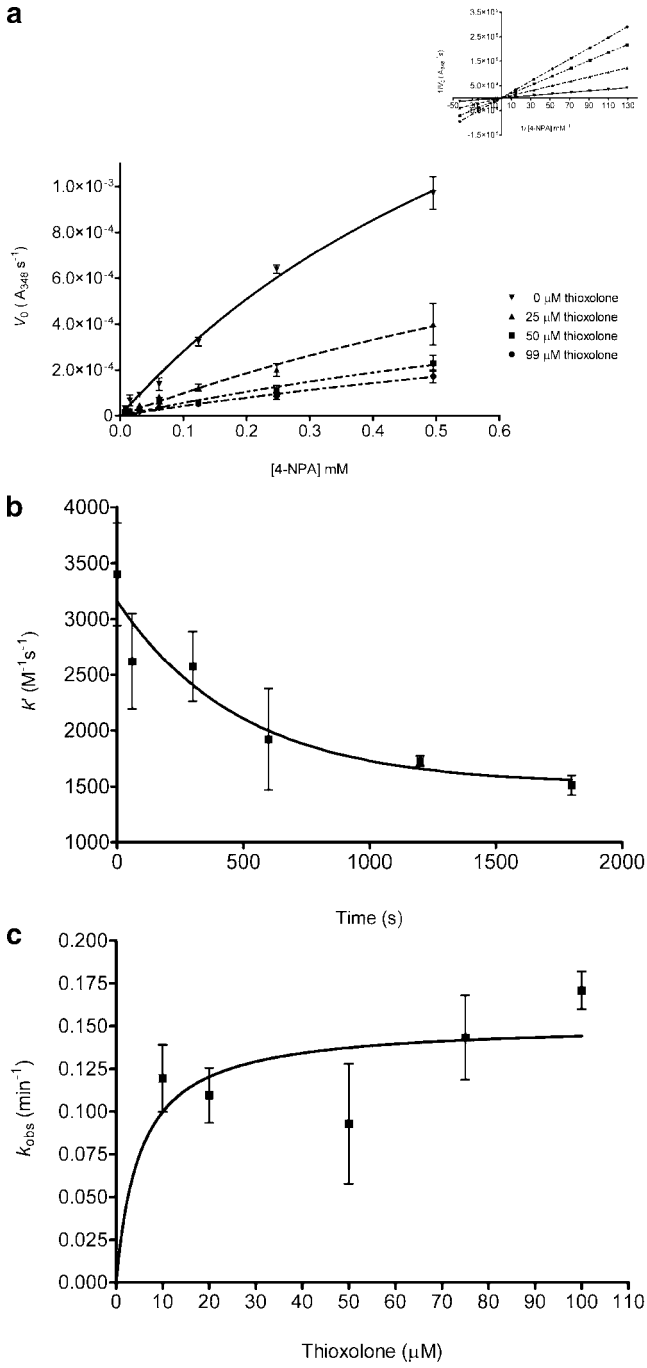

FIGURE 1: Kinetics studies of thioxolone inhibition of CA II esterase activity. (a) The rate of 4-NPA ester hydrolysis catalyzed by CA II as a function of thioxolone concentration. The data was fit to the Michaelis–Menten equation using nonlinear regression analysis and Graphpad Prism 4.03 software. (a) Inset: Lineweaver–Burke plot of the Michaelis–Menten data, indicating apparent mixed inhibition behavior by thioxolone. (b) Time-dependence of thioxolone inhibition of CA II as monitored by apparent second order rate constant, k', as a function of inhibitor incubation time. Data were fit to a single exponential decay model to yield a $t_{1/2}$ value of 340 s. Initial assay conditions were 20 μM thioxolone concentration, 750 μM 4-NPA substrate concentration, and 1 μM CA II. (c) Plot of CA II activity loss versus thioxolone concentration as determined by fitting the decay constant to a nonlinear regression analysis using GraphPad Prism (4.03). Each point is the mean of triplicate data (±SD).

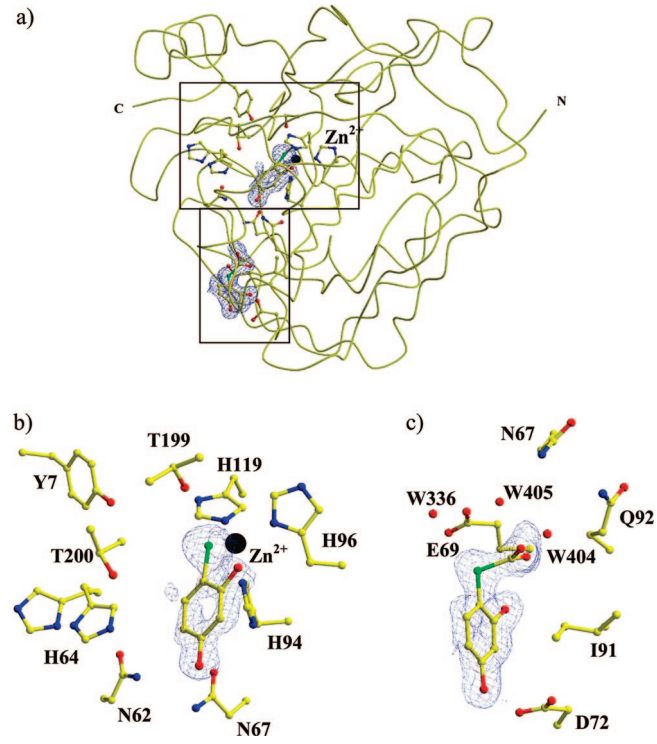

FIGURE 2: Crystal structure of CA II soaked with thioxolone. (a) Ribbon diagram of CA II complexed with (b) 4-mercaptobenzene-1,3-diol (compound **3**) and (c) *S*-(2,4-thiophenyl)hydrogen thiocarbonate; (b) and (c) are close up views of the open boxes as depicted in (a). The zinc atom is shown as a black sphere, and side chains are as labeled. Blue $F_o - F_c$ electron density map shown in (b) and (c) is contoured at 2σ and was calculated without the inhibitors present. Figures were generated and rendered with BobScript and Raster3D, respectively (*95, 96*).

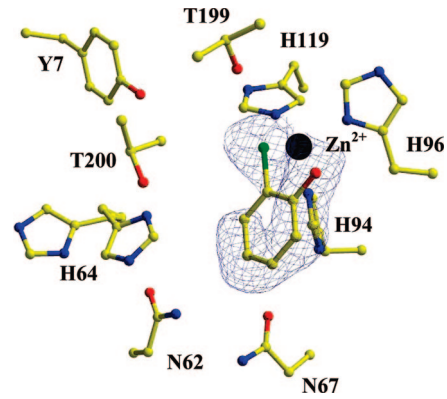

FIGURE 3: Crystal structure of CA II complexed with 2-hydroxythiophenol (compound **4**). The zinc atom is shown as a black sphere, and side chains are as labeled. Blue $F_o - F_c$ electron density map shown is contoured at 2σ and was calculated without the inhibitor present. Figure was generated and rendered with BobScript and Raster3D, respectively (*95, 96*).

confirmed the binding site of 4-mercaptobenzene-1,3-diol (compound **3**) as they were superimposable. The crystallographic studies indicated that the binding mode of the final product of thioxolone hydrolysis, 4-mercaptobenzene-1,3-diol (compound **3**), and the structurally similar analogue 2-hydroxythiophenol (compound **4**), both involve a direct interaction of a thiol group with the zinc ion. This result is not surprising, given that cysteine side chain thiols are one of the four most common zinc ligands in proteins (*83*). Furthermore, this direct interaction with the catalytic zinc ion is similar to the binding mode of other CA sulfonamide and hydroxamate inhibitors, although these other compounds do not have thiols and instead employ an ionized anionic form of the nitrogen atom to bind the zinc ion in the

Table 3: X-ray Crystallographic Data Collection and Structural Refinement Statistics

data set statistics	thioxolone (**1**) soaked CA II crystal	2-hydroxythiophenol (**4**) soaked CA II crystal
unit cell dimensions (*a*, *b*, *c* Å, *β*°)	42.8, 41.7, 72.9, 104.7	42.9, 41.8, 73.1, 104.7
space group	$P2_1$	$P2_1$
resolution range (Å)	2.0−1.6 (1.66–1.60)[c]	20–1.6 (1.66–1.60)
total no. of reflections	88680	76594
unique reflections/redundancy	30612 (2571)/2.9	30184 (2499)/2.5
completeness (%)	92.5 (78.4)	90.6 (75.2)
R_{sym}[a]	0.068 (0.437)	0.134 (0.278)
Model Statistics		
R_{cryst}/R_{free}[b]	0.164/0.211	0.187/0.220
no. protein/solvent/ion/drug atoms	2063/107/1/21	2068/122/1/8
rmsd bond lengths (Å)/angles (°)	0.005/1.39	0.004/1.26
ave B-factor protein main-/side-chain/solvent/drug atoms (Å^2)	18.1/21.3/28.5/30.3	20.5/26.1/42.7/18.7
ave B-factor zinc ion (Å^2)	9.8	15.1
Ramachandran plot statistics (%) Most-favored/allowed	88.4/11.6	88.9/11.1
PDB code	20SF	20SM

[a] $R_{sym} = \Sigma |I - \langle I \rangle| / \Sigma \langle I \rangle$. [b] $R_{cryst} = \Sigma ||F_o| - |F_c|| / \Sigma |F_o|$, R_{free} is calculated the same as R_{cryst}, except it uses 5% of reflection data omitted from refinement. [c] Data in parenthesis are for the highest resolution shell.

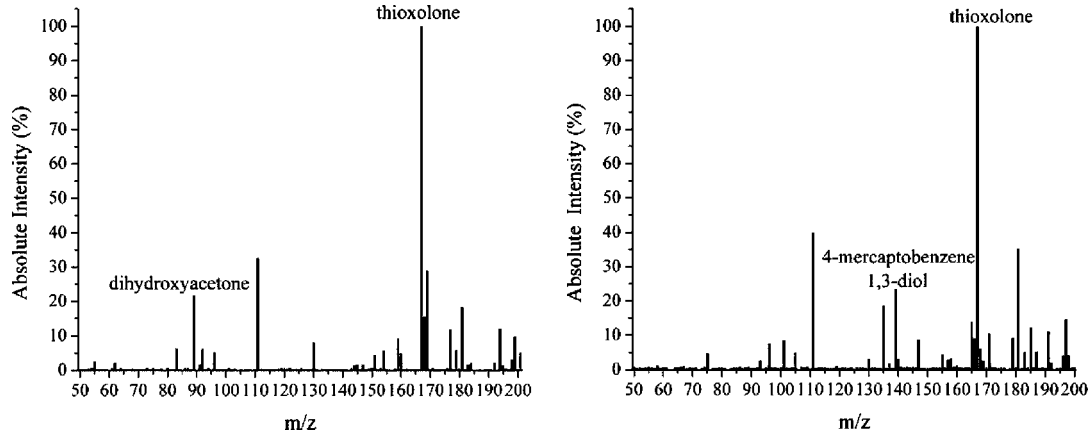

FIGURE 4: LC-MS of thioxolone products generated in the absence and in the presence of CA II. Left, mass spectrum of thioxolone control sample incubated in buffer only. Dihydroxyacetone was also observed in the control sample. Right, mass spectrum of thioxolone and resulting 4-mercaptobenzene-1,3-diol (compound **3**) hydrolysis product observed after thioxolone was incubated with CA II.

sulfonamide, sulfamate, hydroxysulfonamide, or hydroxamate group (*4, 39, 84*). Analyses of various CA−inhibitor cocrystal structures have indicated that the sulfonamide binding mode is generally the same and involves direct coordination of the ionized nitrogen group to the active site zinc (*4, 11*). The deprotonated NH^- group replaces the zinc-bound water molecule and coordinates to the Zn(II) ion. The NH moiety forms hydrogen bonds to the side chain OH group of Thr199, a coordination mechanism termed the "door-keeper" rule for protonated inhibitors, (*4, 11, 17, 25*) and one of the oxygen atoms of the SO_2NH group forms a hydrogen bond with the peptide NH of Thr199. A similar interaction could also occur with 4-mercaptobenzene-1,3-diol (compound **3**) and 2-hydroxythiophenol (compound **4**), where the geometry between Thr199 side chain O atom and the thiophenol S atom indicates that the angle and distance allow for the possibility of a weak hydrogen-bond (Thr199-OH---S) with a distance of 3 Å.

Liquid Chromatography–Mass Spectroscopy Analysis of Thioxolone and Hydrolysis Products. The analytical technique of LC-MS was used to verify that the thioxolone hydrolysis products observed in the preliminary crystal structure were generated by reaction with CA II and were not due to other nonenzymatic hydrolysis events, for example, nonenzymatic cleavage by exposure to X-ray radiation. The LC-MS analysis was first performed in both the positive ionization and negative ionization modes to determine which mode would best detect thioxolone. The negative ionization mode resulted in the detection of the deprotonated thioxolone ion with a mass-to-charge ratio (*m*/*z*) of 167, and the positive mode yielded an *m*/*z* value of 169, as expected. Comparison of the two ionization modes indicated that the negative ionization mode was more sensitive.

Pure thioxolone (compound **1**) was incubated with either CA II enzyme or with enzyme-free buffer as a control; the resulting small molecule products were isolated from the protein by diafiltration and organic liquid–liquid extraction. The resulting products were then analyzed by LC-MS. When thioxolone was incubated with the enzyme, a probable hydrolysis product was isolated with an *m*/*z* value of 139 (Figure 4); this value is consistent with the predicted value for 4-mercaptobenzene-1,3-diol (compound **3**). The amount of 4-mercaptobenzene-1,3-diol in the sample was approximately 23% of the amount of thioxolone present when 5 μM of thioxolone was cleaved by 1 μM CA II. The percentage of 4-mercaptobenzene-1,3-diol to thioxolone was consistently observed in every LC-MS analysis of samples of thioxolone incubated with CA II. The lower *m*/*z* value detected was consistent with the form of 4-mercaptobenzene-1,3-diol resulting from the cleavage of a disulfide-linked dimer, *bis*-4-mercaptobenzene-1,3-diol. When the control

samples of thioxolone without CA II were analyzed by LC-MS, the previous product, 4-mercaptobenzene-1,3-diol (compound **3**), was not detected (Figure 4).

Structure–Activity Relationship Studies of Thioxolone and Structural Analogues. As previously reported, (*1*) thioxolone (compound **1**) is a relatively weak inhibitor of CA II esterase activity, with a measured IC_{50} value of 1.77 μM (Table 1). A preliminary SAR study was performed with a series of small thioxolone structural analogues to examine possible mechanisms of inhibition and determine if the potency of CA II inhibition could be increased (Table 1). The compounds tested included the thioxolone hydrolysis product, 4-mercaptobenzene-1,3-diol (compound **3**) and two smaller structural analogues, 2-hydroxythiophenol (compound **4**) and benzenethiol (compound **5**). Two of these compounds were tested for inhibition of CA II activity, using a 4-NPA esterase assay to determine their inhibition constants. The smaller analogues (compounds **4** and **5**) had IC_{50} values of 1.05 and 1.49 μM, which were slightly lower than thioxolone, with 2-hydroxythiophenol exhibiting greater potency. Thus, the two smaller aromatic thiol compounds appeared to be more potent inhibitors than the parent compound, thioxolone. The IC_{50} values were also similar to those measured for some of the other larger thioxolone analogues, discussed below (Table 1). Inhibition constants (K_i values) of thioxolone (compound **1**), the thioxolone cleavage product, 4-mercaptobenzene-1,3-diol (compound **3**), and 2-hydroxythiophenol (compound **4**) were also determined for the physiologically relevant reaction of CO_2 hydration (Table 1), via titration of the ^{18}O-exchange activity, as monitored by mass spectrometry. This alternate method yielded K_i values of 314 $\pm$ 69 μM, 148 $\pm$ 39 μM, and 0.631 $\pm$ 0.034 μM for compounds **1**, **3**, and **4**, respectively. These results further verified that thioxolone (compound **1**) is a relatively weak inhibitor of CA II activity, whereas the thioxolone hydrolysis product, 4-mercaptobenzene-1,3-diol (compound **3**), although still a relatively weak inhibitor, was 2-fold more potent. In contrast, 2-hydroxythiophenol (compound **4**) showed a significant ~500-fold increase in inhibition, similar in magnitude to other sulfonamide inhibitors. This result suggests that the absence of a second hydroxyl group may have greatly improved the affinity of this molecule in the active site, relative to 4-mercaptobenzene-1,3-diol (compound **3**). A closer examination of the crystal structures of the two complexes (Figures 2, 3) reveals insight into this apparent ~500-fold increase in inhibition of 2-hydroxythiophenol (compound **4**) compared to 4-mercaptobenzene-1,3-diol (compound **3**) on CA II. The additional hydroxyl group of 4-mercaptobenzene-1,3-diol (compound **3**) points toward a hydrophobic pocket in the active site of CA II (in close proximately to residues Ile91, Phe131, Leu141, Val135, and Leu198 - not shown in Figure 2) and this may be the cause of the significant disparity in the affinity of the two compounds. The absence of the second hydroxyl group on the ring of 2-hydroxythiophenol (compound **4**) removes the incompatibility of the hydrophilic nature of this group in the hydrophobic pocket and therefore could explain the greatly improved affinity of this compound.

A preliminary structure–activity relationship (SAR) study was performed on a series of 16 structural analogues of thioxolone (Supporting Information). All 16 analogues contained the original thioxolone ring structure, but also had additional aliphatic and aromatic groups substituted at the C6 carbon hydroxyl group, using the nomenclature of Byres and Cox (*53*). Some analogues were also modified by halogenation of the C1 and/or C5 carbons. Apparent IC_{50} values were determined for these compounds after a 15 min incubation time. Many of these analogues were inhibitory to CA II and yielded apparent IC_{50} magnitudes similar to those of thioxolone, while two compounds were noninhibitory, compounds **6** and **17**. These preliminary observations suggest that the thioxolone ring structure can tolerate additional substitutions at some positions and not others, specifically at the C1 carbon.

To further test this hypothesis, a model was generated of a bromine atom attached to carbon C1 of the thioxolone hydrolysis product, *S*-(2,4-thiophenyl)hydrogen thiocarbonate, in the cocrystal structure. This model indicated a pronounced steric clash between the C1 bromine atom and the CA II active site residue, Val121, providing further support for this hypothesis. Furthermore, bromine present at the C1 position could also reduce the likelihood that hydrolysis of thioxolone compounds would occur, even if binding was feasible. Residue Val121 is one of several residues, along with Val143, Leu198, and Trp209, that function as a hydrophobic pocket for substrate binding, near the zinc-bound hydroxide (*85*). Several studies have shown that these residues are important for the interaction between the enzyme and the 4-NPA substrate (*86–89*) and for specificity for different ester substrates (*52*). Recently, the combination of the two V121A and V143A mutations was shown to greatly increase the rate of CA II hydrolysis of some long chain esters, such as paranitrophenyl valerate (*62*). Thus, it is not unexpected that introducing substituents at certain positions, such as the C1 carbon, could alter the ability of thioxolone analogues to bind in the active site.

It should be noted that none of the 16 analogues tested had any substituents at the C4 carbon; the effect of other functional groups at this position remains to be explored, as does substitution of the reactive ester and thioester bonds with other types of atoms and chemical structures. It also remains to be determined if the addition of sulfonamide and related groups could further improve the potency of thioxolone compounds and what type of inhibition specificity is observed for other alpha class CA isozymes.

DISCUSSION

We have examined the mechanism of thioxolone inhibition of CA II by a variety of analytical and structural methods. The results indicate that thioxolone binds to the active site of CA II and is cleaved by successive hydrolysis of the thioester and ester bonds to form 4-mercaptobenzene-1,3-diol (compound **3**) (Figure 5). The 4-mercaptobenzene-1,3-diol product then binds to the CA II active site zinc ion, displacing the zinc-bound hydroxide group. Thus, thioxolone is proposed to be a prodrug inhibitor that is cleaved via a CA II zinc-hydroxide mechanism known to catalyze the hydrolysis of esters (*52*).

The mechanism of CA II inhibition by thioxolone is complex and cannot be adequately described by simple models of reversible inhibition, as indicated by the failure of Lineweaver–Burke (Figure 1a) and Dixon plot (data not shown) methods of analysis to give a clear mechanistic classification. Suicide inhibitors typically inactivate the

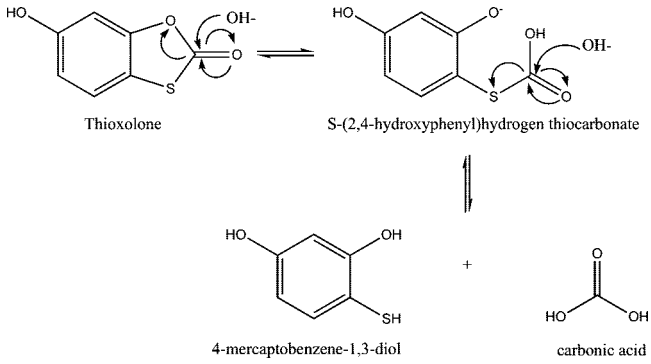

FIGURE 5: Proposed reaction mechanism of thioxolone cleavage by CA II, based on crystallographic studies. The less reactive ester bond is first enzymatically cleaved via nucleophilic attack by the active site Zn-bound hydroxide ion. A second nucleophilic attack by another activated hydroxide ion then cleaves the remaining, more reactive thioester bond, releasing the final inhibitor, 4-mercaptobenzene-1,3-diol (compound **3**) and carbonic acid. The carbonic acid rapidly ionizes to form a bicarbonate ion (HCO_3^-) and CO_2.

Table 4: Mechanism-Based Enzyme Inactivation Parameters Determined for Thioxolone Inhibition of 4-Nitrophenyl Acetate Hydrolysis by Carbonic Anhydrase II[a]

Best-Fit Values	
K_{inact} (min^{-1})	0.15
K_I (μM)	5.21
Standard Error	
K_{inact} (min^{-1})	0.02
K_I (μM)	3.83
95% Confidence Interval	
K_{inact} (min^{-1})	0.12 to 0.19
K_I (μM)	−3.22 to 13.6

[a] Measurements of thioxolone inhibition of the 4-NPA esterase reaction were performed using 1 μM CA II, 750 μM 4-NPA and the varying concentrations of thioxolone (10, 20, 50, 75, and 100 μM). GraphPad Prism version 4.03 was used to fit the data.

enzyme completely. However, this was not observed within the time of the experiment (Figure 1b). This result may be due to competition between the 4-NPA substrate and the final inhibition product, 4-mercaptobenzene-1,3-diol, for the active site, preventing complete CA II inactivation, as observed in other dual substrate systems (*90, 91*). The proposed CA II−thioxolone inhibition mechanism requires multiple steps, some of which are irreversible, as described in the following scheme: (1) initial diffusion into the CA II active site and binding by a thioxolone prodrug molecule (compound **1**); (2) subsequent cleavage of ester and thioester bonds in two successive steps; and (3) a second binding event by one of the resulting cleavage products, 4-mercaptobenzene-1,3-diol (compound **3**), to the active site zinc ion. The first step might be expected to involve competitive inhibition, with thioxolone competing with the 4-NPA substrate for the zinc-hydroxide active site region of the enzyme. The sequential ester and thioester hydrolysis reactions in the second step represent essentially irreversible steps. The last event in the proposed mechanism could potentially involve a noncompetitive inhibition mechanism, due to the formation of a metal–thiol bond between the zinc ion and the product, 4-mercaptobenzene-1,3-diol. Some compounds that form metal–thiol bonds are frequently cited as textbook examples of noncompetitive inhibitors; (*92*) these noncompetitive inhibitor systems are sometimes known to exhibit mixed inhibition as well (*93*).

It is well-known that different CA isozymes vary greatly in their ability to cleave esters; for example, CA III has very little esterase activity with 4-NPA compared to CA II (*94*). Because this type of prodrug inhibitor mechanism depends on activation by enzymatic cleavage of ester bonds, this class of inhibitor may have advantages in determining isozyme specificity. Thioxolone lacks the sulfonamide, sulfamate, or related functional groups that are typically found in known CA inhibitors and could represent the starting point for a new class of CA inhibitors that may have advantages for patients with sulfonamide allergies.

ACKNOWLEDGMENT

The loan of equipment by Procter and Gamble Pharmaceuticals and financial support by the Monroe-Brown Foundation are also gratefully acknowledged.

SUPPORTING INFORMATION AVAILABLE

A detailed description of the synthesis procedures used to prepare 4-mercaptobenzene-1,3-diol and three thioxolone analogues, compounds **19**–**21** and a table of structures and apparent inhibition constants for thioxolone analogues **6**–**21** are available at http://pubs.acs.org.

REFERENCES

1. Iyer, R., Barrese, A. A., 3rd, Parakh, S., Parker, C. N., and Tripp, B. C. (2006) Inhibition profiling of human carbonic anhydrase II by high-throughput screening of structurally diverse, biologically active compounds. *J. Biomol. Screening 11*, 782–791.
2. Tripp, B. C., Smith, K., and Ferry, J. G. (2001) Carbonic anhydrase: new insights for an ancient enzyme. *J. Biol. Chem. 276*, 48615–48618.
3. Lindskog, S., and Silverman, D. N. (2000) The catalytic mechanism of mammalian carbonic anhydrases. *EXS* 175–195.
4. Lindskog, S. (1997) Structure and mechanism of carbonic anhydrase. *Pharmacol. Ther. 74*, 1–20.
5. Khalifah, R. G. (2003) Reflections on Edsall's carbonic anhydrase: paradoxes of an ultra fast enzyme. *Biophys. Chem. 100*, 159–170.
6. Tripp, B. C., Bell, C. B., 3rd, Cruz, F., Krebs, C., and Ferry, J. G. (2004) A role for iron in an ancient carbonic anhydrase. *J. Biol. Chem. 279*, 6683–6687.
7. Lane, T. W., Saito, M. A., George, G. N., Pickering, I. J., Prince, R. C., and Morel, F. M. (2005) Biochemistry: a cadmium enzyme from a marine diatom. *Nature 435*, 42.
8. Lane, T. W., and Morel, F. M. (2000) A biological function for cadmium in marine diatoms. *Proc. Natl. Acad. Sci. U. S. A. 97*, 4627–4631.
9. Smith, K. S., Jakubzick, C., Whittam, T. S., and Ferry, J. G. (1999) Carbonic anhydrase is an ancient enzyme widespread in prokaryotes. *Proc. Natl. Acad. Sci. U. S. A. 96*, 15184–15189.
10. Smith, K. S., and Ferry, J. G. (2000) Prokaryotic carbonic anhydrases. *FEMS Microbiol. Rev. 24*, 335–366.
11. Supuran, C. T., Scozzafava, A., and Conway, J. (2004) *Carbonic Anhydrase. Its Inhibitors and Activators.*, Vol. 1, CRC Press, New York.
12. So, A. K., Espie, G. S., Williams, E. B., Shively, J. M., Heinhorst, S., and Cannon, G. C. (2004) A novel evolutionary lineage of carbonic anhydrase (epsilon class) is a component of the carboxysome shell. *J. Bacteriol. 186*, 623–630.
13. Cox, E. H., McLendon, G. L., Morel, F. M., Lane, T. W., Prince, R. C., Pickering, I. J., and George, G. N. (2000) The active site structure of *Thalassiosira weissflogii* carbonic anhydrase 1. *Biochemistry 39*, 12128–12130.
14. Lane, T. W., and Morel, F. M. (2000) Regulation of carbonic anhydrase expression by zinc, cobalt, and carbon dioxide in the marine diatom *Thalassiosira weissflogii*. *Plant Physiol. 123*, 345–352.

15. Zimmerman, S. A., Ferry, J. G., and Supuran, C. T. (2007) Inhibition of the archaeal beta-class (Cab) and gamma-class (Cam) carbonic anhydrases. *Curr. Top. Med. Chem. 7*, 901–908.
16. Saarnio, J. (2000) in Departments of Surgery, Anatomy and Cell Biology and Pathology p 80, University of Oulu, Oulu, Finland.
17. Supuran, C. T., Scozzafava, A., and Casini, A. (2003) Carbonic anhydrase inhibitors. *Med. Res. Rev. 23*, 146–189.
18. Pastorekova, S., Parkkila, S., Pastorek, J., and Supuran, C. T. (2004) Carbonic anhydrases: current state of the art, therapeutic applications and future prospects. *J. Enzyme Inhib. Med. Chem. 19*, 199–229.
19. Stadie, W. C., and O-Brien, H. (1933) The catalysis of the hydration of carbon dioxide and dehydration of carbonic acid by an enzyme isolated from red blood cells. *J. Biol. Chem. 103*, 521–529.
20. Meldrum, N. U., and Roughton, F. J. (1933) Carbonic anhydrase, its preparation and properties. *J. Physiol. 80*, 113–142.
21. Khalifah, R. G. (1971) The carbon dioxide hydration activity of carbonic anhydrase I. Stop-flow kinetic studies on the native human isoenzymes B and C. *J. Biol. Chem. 246*, 2561–2573.
22. Maren, T. H., and Conroy, C. W. (1993) A new class of carbonic anhydrase inhibitor. *J. Biol. Chem. 268*, 26233–26239.
23. Supuran, C. T., and Scozzafava, A. (2002) Applications of carbonic anhydrase inhibitors and activators in therapy. *Expert Opin. Ther. Pat. 12*, 217–241.
24. Maren, T. H. (1967) Carbonic anhydrase - chemistry physiology and inhibition. *Physiol. Rev. 47*, 595.
25. Supuran, C. T., and Scozzafava, A. (2000) Carbonic anhydrase inhibitors and their therapeutic potential. *Expert Opin. Ther. Pat. 10*, 575–600.
26. Richalet, J. P., Rivera, M., Bouchet, P., Chirinos, E., Onnen, I., Petitjean, O., Bienvenu, A., Lasne, F., Moutereau, S., and Leon-Velarde, F. (2005) Acetazolamide: a treatment for chronic mountain sickness. *Am. J. Respir. Crit. Care Med. 172*, 1427–1433.
27. Supuran, C. T., Briganti, F., Tilli, S., Chegwidden, W. R., and Scozzafava, A. (2001) Carbonic anhydrase inhibitors: Sulfonamides as antitumor agents? *Bioorg. Med. Chem. 9*, 703–714.
28. Sanders, E., and Maren, T. H. (1967) Inhibition of carbonic anhydrase in Neisseria: effects on enzyme activity and growth. *Mol. Pharmacol. 3*, 204–215.
29. Huang, S., Xue, Y., Sauer-Eriksson, E., Chirica, L., Lindskog, S., and Jonsson, B. H. (1998) Crystal structure of carbonic anhydrase from *Neisseria gonorrhoeae* and its complex with the inhibitor acetazolamide. *J. Mol. Biol. 283*, 301–310.
30. Elleby, B., Chirica, L. C., Tu, C., Zeppezauer, M., and Lindskog, S. (2001) Characterization of carbonic anhydrase from Neisseria gonorrhoeae. *Eur. J. Biochem. 268*, 1613–1619.
31. Chirica, L. C., Elleby, B., and Lindskog, S. (2001) Cloning, expression and some properties of alpha-carbonic anhydrase from *Helicobacter pylori*. *Biochim. Biophys. Acta 1544*, 55–63.
32. Nishimori, I., Vullo, D., Minakuchi, T., Morimoto, K., Onishi, S., Scozzafava, A., and Supuran, C. T. (2006) Carbonic anhydrase inhibitors: cloning and sulfonamide inhibition studies of a carboxyterminal truncated alpha-carbonic anhydrase from *Helicobacter pylori*. *Bioorg. Med. Chem. Lett. 16*, 2182–2188.
33. Nishimori, I., Minakuchi, T., Morimoto, K., Sano, S., Onishi, S., Takeuchi, H., Vullo, D., Scozzafava, A., and Supuran, C. T. (2006) Carbonic anhydrase inhibitors: DNA cloning and inhibition studies of the alpha-carbonic anhydrase from *Helicobacter pylori*, a new target for developing sulfonamide and sulfamate gastric drugs. *J. Med. Chem. 49*, 2117–2126.
34. Reungprapavut, S., Krungkrai, S. R., and Krungkrai, J. (2004) *Plasmodium falciparum* carbonic anhydrase is a possible target for malaria chemotherapy. *J. Enzyme Inhib. Med. Chem 19*, 249–256.
35. Krungkrai, J., Scozzafava, A., Reungprapavut, S., Krungkrai, S. R., Rattanajak, R., Kamchonwongpaisan, S., and Supuran, C. T. (2005) Carbonic anhydrase inhibitors. Inhibition of Plasmodium falciparum carbonic anhydrase with aromatic sulfonamides: towards antimalarials with a novel mechanism of action? *Bioorg. Med. Chem. 13*, 483–489.
36. Sein, K. K., and Aikawa, M. (1998) The pivotal role of carbonic anhydrase in malaria infection. *Med. Hypotheses 50*, 19–23.
37. Mann, B., and Keilin, D. (1940) Sulphanilamide as a specific inhibitor of carbonic anhydrase. *Nature 146*, 164–165.
38. Supuran, C. T., Vullo, D., Manole, G., Casini, A., and Scozzafava, A. (2004) Designing of novel carbonic anhydrase inhibitors and activators. *Curr. Med. Chem. Cardiovasc. Hematol. Agents 2*, 49–68.
39. Winum, J. Y., Scozzafava, A., Montero, J. L., and Supuran, C. T. (2006) New zinc binding motifs in the design of selective carbonic anhydrase inhibitors. *Mini Rev. Med. Chem. 6*, 921–936.
40. Scolnick, L. R., Clements, A. M., Liao, J., Crenshaw, L., Hellberg, M., May, J., Dean, T. R., and Christianson, D. W. (1997) Novel binding mode of hydroxamate inhibitors to human carbonic anhydrase II. *J. Am. Chem. Soc. 119*, 850–851.
41. Winum, J. Y., Scozzafava, A., Montero, J. L., and Supuran, C. T. (2005) Sulfamates and their therapeutic potential. *Med. Res. Rev. 25*, 186–228.
42. Epstein, D. L., and Grant, W. M. (1977) Carbonic anhydrase inhibitor side effects. Serum chemical analysis. *Arch. Ophthalmol. 95*, 1378–1382.
43. Wallace, T. R., Fraunfelder, F. T., Petursson, G. J., and Epstein, D. L. (1979) Decreased libido-a side effect of carbonic anhydrase inhibitor. *Ann. Ophthalmol. 11*, 1563–1566.
44. Lichter, P. R., Newman, L. P., Wheeler, N. C., and Beall, O. V. (1978) Patient tolerance to carbonic anhydrase inhibitors. *Am. J. Opthalmol. 85*, 495–502.
45. Lichter, P. R. (1981) Reducing side effects of carbonic anhydrase inhibitors. *Ophthalmology 88*, 266–269.
46. Saxon, A., and Macy, E. (2004) Cross-reactivity and sulfonamide antibiotics. *N. Engl. J. Med. 350*, 302303; author reply pp 302–303.
47. Ray, W. A. (2003) Population-based studies of adverse drug effects. *N. Engl. J. Med. 349*, 1592–1594.
48. Strom, B. L., Schinnar, R., Apter, A. J., Margolis, D. J., Lautenbach, E., Hennessy, S., Bilker, W. B., and Pettitt, D. (2003) Absence of cross-reactivity between sulfonamide antibiotics and sulfonamide nonantibiotics. *N. Engl. J. Med. 349*, 1628–1635.
49. Pocker, Y., and Stone, J. T. (1967) The catalytic versatility of erythrocyte carbonic anhydrase. 3. Kinetic studies of the enzyme-catalyzed hydrolysis of *p*-nitrophenyl acetate. *Biochemistry 6*, 668–678.
50. Verpoorte, J. A., Mehta, S., and Edsall, J. T. (1967) Esterase activities of human carbonic anhydrases B and C. *J. Biol. Chem. 242*, 4221–4229.
51. Pocker, Y., and Sarkanen, S. (1978) Carbonic anhydrase: structure catalytic versatility, and inhibition. *Adv. Enzymol. Relat. Areas Mol. Biol. 47*, 149–274.
52. Elleby, B., Sjoblom, B., and Lindskog, S. (1999) Changing the efficiency and specificity of the esterase activity of human carbonic anhydrase II by site-specific mutagenesis. *Eur. J. Biochem. 262*, 516–521.
53. Byres, M., and Cox, P. J. (2004) The supramolecular structure of 6-hydroxy-1,3-benzoxathiol-2-one (tioxolone). *Acta Crystallogr. C 60*, o395–396.
54. Wildfeuer, A. (1970) [6-Hydroxy-1,3-benzoxathiol-2-one, an antipsoriatic with antibacterial and antimycotic properties]. *Arzneimittelforschung 20*, 824–831.
55. Lius, V., and Sennerfeldt, P. (1979) [Local treatment of acne with tioxolone]. *Lakartidningen 76*, 39–41.
56. Goeth, H., and Wildfeuer, A. (1969) Antibacterial and cytostatic properties of 6-hydroxy-1,3-benzoxathiol-2-one. *Arzneimittelforschung 19*, 1298–1304.
57. Camarasa, J. G. (1981) Contact dermatitis to thioxolone. *Contact Dermatitis 7*, 213–214.
58. Simonsson, I., Jonsson, B. H., and Lindskog, S. (1982) Phenol, a competitive inhibitor of CO2 hydration catalyzed by carbonic anhydrase. *Biochem. Biophys. Res. Commun. 108*, 1406–1412.
59. Tibell, L., Forsman, C., Simonsson, I., and Lindskog, S. (1985) The inhibition of human carbonic anhydrase II by some organic compounds. *Biochim. Biophys. Acta 829*, 202–208.
60. Thorslund, A., and Lindskog, S. (1967) Studies of the esterase activity and the anion inhibition of bovine zinc and cobalt carbonic anhydrases. *Eur. J. Biochem. 3*, 117–123.
61. Gould, S. M., and Tawfik, D. S. (2005) Directed evolution of the promiscuous esterase activity of carbonic anhydrase II. *Biochemistry 44*, 5444–5452.
62. Host, G., Martensson, L. G., and Jonsson, B. H. (2006) Redesign of human carbonic anhydrase II for increased esterase activity and specificity towards esters with long acyl chains. *Biochim. Biophys. Acta 1764*, 1601–1606.
63. Bergmann, F., Rimon, S., and Segal, R. (1958) Effect of pH on the activity of eel esterase towards different substrates. *Biochem. J. 68*, 493–499.
64. Armstrong, J. M., Myers, D. V., Verpoorte, J. A., and Edsall, J. T. (1966) Purification and properties of human erythrocyte carbonic anhydrases. *J. Biol. Chem. 241*, 5137–5149.

65. Baird, T. T., Jr., Waheed, A., Okuyama, T., Sly, W. S., and Fierke, C. A. (1997) Catalysis and inhibition of human carbonic anhydrase IV. *Biochemistry 36*, 2669–2678.
66. Fersht, A. (1999) *Structure and Mechanism in Protein Science: A Guide to Enzyme Catalysis and Protein Folding*, W. H. Freeman and Company, New York.
67. Chang, T. K., Chen, J., and Lee, W. B. (2001) Differential inhibition and inactivation of human CYP1 enzymes by trans-resveratrol: evidence for mechanism-based inactivation of CYP1A2. *J. Pharmacol. Exp. Ther. 299*, 874–882.
68. Maurer, T., and Fung, H. L. (2000) Comparison of methods for analyzing kinetic data from mechanism-based enzyme inactivation: application to nitric oxide synthase. *AAPS PharmSci 2*, E8.
69. Silverman, D. N. (1982) Carbonic anhydrase: oxygen-18 exchange catalyzed by an enzyme with rate-contributing proton-transfer steps. *Methods Enzymol. 87*, 732–752.
70. Fisher, Z., HernandezPrada, J. A., Tu, C., Duda, D., Yoshioka, C., An, H., Govindasamy, L., Silverman, D. N., and McKenna, R. (2005) Structural and kinetic characterization of active-site histidine as a proton shuttle in catalysis by human carbonic anhydrase II. *Biochemistry 44*, 1097–1105.
71. Segel, I. H. (1975) Enzyme Kinetics: Behavior and Analysis of Rapid Equilibrium and Steady-State Enzyme Systems, Wiley-Interscience, New York.
72. McPherson, A. (1982) *Preparation and Analysis of Protein Crystals*, John Wiley and Sons, New York.
73. Otwinowski, Z., and Minor, W. (1997) Processing of X-ray Diffraction Data Collected in Oscillation Mode. *Methods Enzymol. 276*, 307–326.
74. Rossmann, M. G. (1990) The molecular replacement method. *Acta Crystallogr. A 46(Pt 2)* , 73–82.
75. Brunger, A. T., Adams, P. D., Clore, G. M., DeLano, W. L., Gros, P., Grosse-Kunstleve, R. W., Jiang, J. S., Kuszewski, J., Nilges, M., Pannu, N. S., Read, R. J., Rice, L. M., Simonson, T., and Warren, G. L. (1998) Crystallography & NMR system: A new software suite for macromolecular structure determination. *Acta Crystallogr. D Biol. Crystallogr. 54*, 905–921.
76. Emsley, P., and Cowtan, K. (2004) Coot: model-building tools for molecular graphics. *Acta Crystallogr. D Biol. Crystallogr. 60*, 2126–2132.
77. Schuttelkopf, A. W., and van Aalten, D. M. (2004) PRODRG: a tool for high-throughput crystallography of protein-ligand complexes. *Acta Crystallogr. D Biol. Crystallogr. 60*, 1355–1363.
78. Sheldrick, G. M., and Schneider, T. R. (1997) SHELXL: High Resolution Refinement. *Methods Enzymol. 277*, 319–343.
79. Laskowski, R. A., MacArthur, M. W., Moss, D. S., and Thornton, J. M. (1993) PROCHECK: A program to check the stereochemical quality of protein structures. *J. Appl. Crystallogr. 26*, 283–291.
80. Wallace, A. C., Laskowski, R. A., and Thornton, J. M. (1995) LIGPLOT: a program to generate schematic diagrams of protein-ligand interactions. *Protein Eng. 8*, 127–134.
81. Banerjee, A. L., Swanson, M., Roy, B. C., Jia, X., Haldar, M. K., Mallik, S., and Srivastava, D. K. (2004) Protein surface-assisted enhancement in the binding affinity of an inhibitor for recombinant human carbonic anhydrase-II. *J. Am. Chem. Soc. 126*, 10875–10883.
82. Copeland, R. A. (2003) Mechanistic considerations in high-throughput screening. *Anal. Biochem. 320*, 1–12.
83. Auld, D. S. (2001) Zinc coordination sphere in biochemical zinc sites. *Biometals 14*, 271–313.
84. Winum, J. Y., Scozzafava, A., Montero, J. L., and Supuran, C. T. (2007) Metal binding functions in the design of carbonic anhydrase inhibitors. *Curr. Top. Med. Chem. 7*, 835–848.
85. Eriksson, A. E., Jones, T. A., and Liljas, A. (1988) Refined structure of human carbonic anhydrase II at 20 Å resolution. *Proteins 4*, 274–282.
86. Fierke, C. A., Calderone, T. L., and Krebs, J. F. (1991) Functional consequences of engineering the hydrophobic pocket of carbonic anhydrase II. *Biochemistry 30*, 11054–11063.
87. Nair, S. K., Calderone, T. L., Christianson, D. W., and Fierke, C. A. (1991) Altering the mouth of a hydrophobic pocket. Structure and kinetics of human carbonic anhydrase II mutants at residue Val-121. *J. Biol. Chem. 266*, 17320–17325.
88. Krebs, J. F., Rana, F., Dluhy, R. A., and Fierke, C. A. (1993) Kinetic and spectroscopic studies of hydrophilic amino acid substitutions in the hydrophobic pocket of human carbonic anhydrase II. *Biochemistry 32*, 4496–4505.
89. Krebs, J. F., and Fierke, C. A. (1993) Determinants of catalytic activity and stability of carbonic anhydrase II as revealed by random mutagenesis. *J. Biol. Chem. 268*, 948–954.
90. Wimalasena, K., and Haines, D. C. (1996) A general progress curve method for the kinetic analysis of suicide enzyme inhibitors. *Anal. Biochem. 234*, 175–182.
91. Moruno-Davila, M. A., Garrido-del Solo, C., Garcia-Moreno, M., Havsteen, B. H., Garcia-Sevilla, F., Garcia-Canovas, F., and Varon, R. (2001) Kinetic analysis of enzyme systems with suicide substrate in the presence of a reversible competitive inhibitor, tested by simulated progress curves. *Int. J. Biochem. Cell Biol. 33*, 181–191.
92. Berg, J. M., Tymoczko, J. L., and Stryer, L. (2007) *Biochemistry*, 6th ed., W. H. Freeman, New York.
93. Boyer, R. F. (2006) *Concepts in Biochemistry*, 3rd ed., John Wiley and Sons, Hoboken, NJ.
94. Jewell, D. A., Tu, C. K., Paranawithana, S. R., Tanhauser, S. M., LoGrasso, P. V., Laipis, P. J., and Silverman, D. N. (1991) Enhancement of the catalytic properties of human carbonic anhydrase III by site-directed mutagenesis. *Biochemistry 30*, 1484–1490.
95. Esnouf, R. M. (1997) An extensively modified version of MolScript that includes greatly enhanced coloring capabilities. *J. Mol. Graph. Model. 15*, 132–134, 112–113.
96. Merritt, E. A., and Bacon, D. J. (1997) Raster 3D Version 2: photorealistic molecular graphics. *Methods Enzymol. 277*, 505–524.

BI702385K